RNA interference in meiosis I human oocytes: towards an understanding of human aneuploidy

Hayden A Homer, Alex Mcdougall, Mark Levasseur, Alison P Murdoch, Mary Herbert

 doi:10.1093/molehr/gah184

Mol. Hum. Reprod. Advance Access published May 20, 2005

RNA interference in meiosis I human oocytes: towards an understanding of human aneuploidy

Hayden A.Homer[1,2,5], Alex McDougall[2,4], Mark Levasseur[2], Alison P.Murdoch[1,3] and Mary Herbert[1,3,5]

[1]Newcastle Fertility Centre at Life, International Centre for Life, Times Square, Newcastle upon Tyne NE1 4EP, [2]School of Cell and Molecular Biosciences and [3]School of Surgical and Reproductive Sciences, The Medical School, Framlington Place, University of Newcastle, Newcastle upon Tyne NE2 4HH, UK

[4]Present address: UMR 7009 CNRS/Université Pierre et Marie Curie (Paris VI), Observetoire Océanologique, 06230 Villefranche-sur-Mer, France

[5]To whom correspondence should be addressed at: Wansbeck General Hospital, Woodhorn Lane, Ashington, Northumberland NE63 9JJ, UK. E-mail: h.a.homer@ncl.ac.uk

Although female meiosis I errors account for the majority of human aneuploidy, their molecular basis is largely unknown. By elucidating gene function, gene knockdown using RNA interference (RNAi) could shed light on this enigmatic process. In practice, however, the extreme paucity of immature human oocytes makes the evaluation of gene-targeting tools difficult. Here, we undertake RNAi in human oocytes and describe an approach employing mouse oocytes which could overcome the problem of limited biological material. We designed a short interfering RNA (siRNA) designated si539 to target the human mitotic arrest deficient 2 (hMad2) spindle checkpoint component. In human oocytes microinjected with si539, the hMad2 signal detected by Western blotting was 85–92% less intense than in oocytes injected with control siRNA indicating efficient silencing. Further examination of si539's targeting efficiency was undertaken using a green fluorescent protein (GFP)-tagged hMad2 mRNA construct in mouse oocytes. Consistent with Western blot analysis, si539 reduced hMad2-GFP expression in mouse oocytes by ~94% and relieved the meiosis I arrest otherwise induced by hMad2-GFP in mouse oocytes. By facilitating the investigation of candidate genes involved in regulating human female meiosis I, this approach can bring us closer to understanding the origins of aneuploidies such as Down's syndrome.

Key words: green fluorescent protein/Mad2/meiosis I/oocytes/RNA interference

Introduction

The overwhelming majority of human aneuploidy arises from errors that occur when recombined homologous chromosomes segregate or 'disjoin' during meiosis I in oocytes (Hassold and Hunt, 2001). As women age, embryonic aneuploidy due to meiosis I errors occur with increasing frequency resulting in higher risks of miscarriage and chromosomal abnormalities such as Down's syndrome (Hassold and Hunt, 2001). In spite of this, surprisingly little is known about the molecular details involved in regulating homologue disjunction in human oocytes. This is in large part due to the limited supply of immature human oocytes available for research making the application of techniques for the elucidation of gene function difficult.

An established approach for defining the function of a particular gene involves studying the effects produced when that gene is suppressed. In recent years, gene expression has become more widely amenable to down-regulation in mammalian cells by the technique of RNA interference (RNAi) (see for review, Dykxhoorn *et al.*, 2003). RNAi is a powerful new technology that provides rapid suppression of a specific gene through double-stranded (ds) short interfering RNAs (siRNAs) (Elbashir *et al.*, 2001). siRNAs are 21–23-nucleotide (nt) dsRNAs that target complementary mRNA for degradation by acting as a guide sequence within a multi-component nuclease complex called the RNA-induced silencing complex (Dykxhoorn *et al.*, 2003). Mouse oocytes have been shown to possess the machinery for RNAi-mediated gene suppression using long dsRNAs (Svoboda *et al.*, 2000; Wianny and Zernicka-Goetz, 2000; Lefebvre *et al.*, 2002), siRNAs (Kim *et al.*, 2002; Stein *et al.*, 2003a) and long hairpin RNAs expressed from transgenes (Stein *et al.*, 2003b; Fedoriw *et al.*, 2004; Yu *et al.*, 2004).

One approach for exploring how human oocytes regulate homologue disjunction would be to apply RNAi to genes shown to be required for accurate chromosome segregation during meiosis I in other species. One such group of genes encodes for proteins of the spindle checkpoint surveillance system. The spindle checkpoint has long been known to be essential for accurate chromosome segregation during mitosis (see for review, Mussachio and Hardwick, 2002). More recently, the spindle checkpoint has also been shown to be essential for the fidelity of homologue disjunction in a variety of species including yeast (Shonn *et al.*, 2000; Bernard *et al.*, 2001), zebrafish (Poss *et al.*, 2004) and mouse oocytes (Homer *et al.*, 2005). This checkpoint is comprised primarily of the mitotic arrest deficient (Mad) and the budding uninhibited by benzimidazole (Bub) protein families (Mussachio and Hardwick, 2002). In the presence of misaligned chromosomes, checkpoint proteins such as Mad2 and BubR1 (the vertebrate homologue of yeast Mad3) prevent anaphase by inhibiting a multi-subunit protein complex called the

anaphase-promoting complex/cyclosome (APC/C) (Peters, 2002). Following proper chromosome alignment, checkpoint-induced inhibition is relieved and APC/C-mediated destruction of key proteins such as securin and cyclin B1 initiate anaphase (Peters, 2002).

Human oocytes have been shown to possess transcripts encoding Mad2 (Steuerwald *et al.*, 2001) and to express Mad2 protein (Homer *et al.*, 2005). As it appears that the level of transcripts encoding checkpoint proteins decreases in oocytes with advancing maternal age (Steuerwald *et al.*, 2001), it is tempting to speculate that declining oocyte spindle checkpoint function could contribute to the observed rise in aneuploidy as women get older. Definitive testing of this hypothesis requires that spindle checkpoint gene function be characterized in human oocytes.

Although RNAi has been demonstrated to be a viable option for gene knockdown in mouse oocytes and more recently in human endometrial cells (Tulac *et al.*, 2004), its feasibility in human oocytes is untested. Herein, we show by Western blotting that human Mad2 (hMad2) can be silenced in human oocytes using an siRNA which we designated si539. As further proof of concept we show that si539 suppressed expression from a hMad2-green fluorescent protein (GFP) mRNA construct in mouse oocytes. By reducing the number of human oocytes required during the evaluation phase of RNAi, this model may provide a more general framework for investigating human female meiosis I gene regulation.

Materials and methods

Acquisition and culture of human oocytes

Immature oocytes were obtained from consenting women undergoing ICSI at the Newcastle Fertility Centre following ovarian stimulation using a standard regime (Fenwick *et al.*, 2002). Women scheduled for ICSI were counselled at the time of their final ultrasound scan and given a printed information leaflet. Written consent was sought 2–3 days later on the morning of oocyte retrieval. The project was approved by the Local Research Ethics Committee.

Following removal of cumulus cells, oocyte maturation status was evaluated by light microscopy. Immature oocytes (which are not used for infertility treatment) were identified by the presence of a germinal vesicle (GV) and allocated to this research project. GV-stage oocytes were cultured in microdrops of pre-warmed (37°C) G-MOPS medium (Vitrolife, Research Instruments Ltd, Cornwall, UK) supplemented with 50 μg/ml dibutyryl cyclic AMP (dbcAMP) which prevents oocytes from undergoing germinal vesicle breakdown (GVBD). Oocytes were maintained at the GV-stage until microinjection was undertaken about 1–2 h later.

Collection, culture and drug treatment of mouse oocytes

Ovaries were isolated from 4–6-week-old female MF1 mice 46–48 h after treatment with 7.5–10 IU of pregnant mare's serum gonadotrophin. Ovaries were placed in a Petri dish with pre-warmed (37°C) M2 medium (Sigma, Poole, UK) supplemented with 50 μg/ml dbcAMP. Oocytes were released by puncturing antral follicles with a fine needle on the stage of a dissecting microscope. Only fully grown, GV-intact oocytes were utilized for further experiments.

Microinjection

Holding and injection pipettes were made from sterile filament-free GC100T-10 glass (Clarke Electromedical Instruments, Berkshire, UK) using a P-97 micropipette puller (Sutter Instrument Co., Novato, CA, USA) following which they were angled at approximately 50° using a microforge (Research Instruments, Cornwall, UK). Microinjections were carried out on a Nikon Diaphot ECLIPSE TE 300 inverted microscope (Nikon UK Ltd, Surrey, UK) equipped with Narishige MM0-202N hydraulic three-dimensional micromanipulators (Narishige, Inc., Sea Cliff, NY, USA) using a 10×/0.25 n.a. objective combined with a 2.5× magnifier. About 1 μl of test solutions was micropipetted into capillary tubes and sandwiched between oil to reduce evaporation and loaded tubes were mounted onto glass slides using paraffin wax. Injection micropipettes were introduced across the oil layer into the solution and tip-filled by reducing the balance pressure using a semi-automatic Narishige IM 300 microinjection device (Narishige, Inc., Sea Cliff, NY, USA). After filling, the meniscus was stabilized by adjusting the balance pressure. GV-stage oocytes were immobilized using a holding pipette and the tip of the injection pipette was introduced across the zona pellucida and oolemma into the ooplasm. A pressure pulse was applied (4–10 psi) to microinject test solutions (either mRNAs or siRNAs) equivalent to ~5% of the total oocyte volume. The concentrations of microinjected test solutions are indicated below.

GV-stage mouse and human oocytes were microinjected in droplets of pre-warmed dbcAMP-supplemented G-MOPS or M2 medium under mineral oil, respectively (Sigma, Poole, UK). Following microinjection, human oocytes were transferred to fresh G-MOPS, and mouse oocytes were transferred to fresh M2 medium to allow recovery for at least 30 min. Human oocytes were then transferred to microdrops of G-SPERM medium (Vitrolife) and mouse oocytes to microdrops of M16 medium (Sigma, Poole, UK) under mineral oil for longer term culture at 37°C in a humidified atmosphere of 5% CO_2 in air.

In the absence of dbcAMP, the majority of oocytes spontaneously undergo GVBD which marks the resumption of meiosis I. For mouse oocytes utilized for time-lapse experiments, culture was undertaken within a stage-mounted Perspex incubator (see below) while oocytes (including all human oocytes) that were earmarked for other experiments were maintained in a standard laboratory CO_2 incubator. For the latter group of oocytes, the time of GVBD was determined by briefly examining oocytes under the light microscope at half-hourly intervals from the commencement of culture. In the case of time-lapse experiments in which frames were captured at 20 min intervals (see below), GVBD was easily identifiable as the frame at which the GV was no longer visible (Figure 4A and C).

GFP and hMad2-GFP mRNA constructs

GFP mRNA was produced from the pMDL2 transcription vector. The pMDL2 vector was derived from the pRN3 vector (Lemaire *et al.*, 1995) by subcloning the sequence for MmGFP between the *Eco*RI and the *Not*I sites and incorporates an additional *Sal*I site at the 5′ end of MmGFP. MmGFP represents a mutated form of the wild-type protein which is 50-fold brighter and is an enduring marker when microinjected into mouse cells in the form of mRNA transcripts (Zernicka-Goetz *et al.*, 1997). The pRN3 vector allows *in vitro* transcription of mRNA from a T3 promoter with maximal stability conferred by the presence of a 5′ globin untranslated region (UTR) upstream and both a 3′ UTR and a poly(A)-encoding tract downstream of the gene to be transcribed. To construct hMad2-GFP, full-length sequence coding for *hMad2* was subcloned into the pMDL2 transcription vector between the *Sal*I and the *Eco*RI sites. Capped mRNA consisting of either MmGFP alone or hMad2 fused via its C-terminus through a 5-amino acid linker (AGAQF) to the second N-terminal amino acid residue of MmGFP (Figure 3A) was produced using the T3 mMESSAGE mMACHINE kit (Ambion, Inc., Austin, TX, USA) and dissolved in nuclease-free water to a final concentration of 1–1.5 μg/μl. Oocytes were microinjected with ~1 μg/μl of either GFP mRNA or hMad2-GFP mRNA in amounts which equated to ~5% total oocyte volume. Polyadenylation is a major factor that determines the efficiency of expression of injected mRNA in mouse oocytes (Ledan *et al.*, 2001). We have found the length of the poly(A) tail in our GFP and hMad2-GFP mRNA constructs to be conducive to efficient and reliable translation in mouse oocytes (Homer *et al.*, 2005).

Immunoblotting

Oocyte samples were collected in sample buffer containing β-mercaptoethanol and immediately frozen at −20°C. Following thaw, samples were heated to 95°C for 5 min and proteins were resolved by standard SDS-polyacrylamide gel electrophoresis on a 12% gel and electrically transferred to a hydrophobic polyvinylidene difluoride membrane (Hybond-P; Amersham Biosciences, Buckinghamshire, UK). Following transfer, non-specific binding sites were blocked by incubating membranes for 2 h in 5% non-fat milk in Tris-buffered saline (TBS) (25 mM Tris, 150 mM NaCl, pH 8) containing 0.05% Tween 20 (TBST). Membranes were first probed with the goat polyclonal antibody against Mad2 (sc-6330; Santa Cruz Biotechnology, Inc.,

Santa Cruz, CA, USA). Following three 5 min washes in TBST, incubation with horse-radish peroxidase-conjugated secondary antibody and a urther three TBST washes and one TBS wash, detection was performed using the ECL Plus chemiluminescence system (Amersham Biosciences, Buckinghamshire, UK) according to the manufacturer's protocol. The same membrane was then directly re-probed with either the mouse monoclonal antibody against GAPDH (ab8245; Abcam Ltd, Cambridge, UK) or the rat monoclonal antibody YL1/2 to tyrosinated α-tubulin (ab6160; Abcam Ltd, Cambridge, UK) as previously described (Liao *et al.*, 2000; Homer *et al.*, 2005). The anti-Mad2 antibody (sc-6330; Santa Cruz Biotechnology, Inc., Santa Cruz, CA, USA) reacted with a conserved epitope located within the N-terminal region of hMad2 and mouse Mad2 (mMad2). Similar results were obtained with an anti-Mad2 antibody directed against a peptide mapping to the C-terminal region of hMad2 (sc-6329; Santa Cruz Biotechnology, Inc., Santa Cruz, CA, USA). Protein expression was examined by analysing the optical density of the bands obtained in each Western blot analysis using TINA software, as described previously (Homer *et al.*, 2005).

Time-lapse imaging and visualization of DNA in live oocytes

Imaging was performed using a Nikon Eclipse TE2000-U inverted fluorescence microscope equipped with 20×/0.75 n.a. and 40×/1.4 n.a. Plan Fluor oil immersion objectives; motorized shutters for brightfield and epifluorescence illumination; motorized excitation and emission filter wheels; dichroic filter blocks for viewing GFP, 4′,6-diamidino-2-phenylindole (for Hoechst 33342-stained DNA), or rhodamine (for propidium iodide-stained DNA) housed in a rotating turret; a Photometrics CoolSnap$_{HQ}$™ interline cooled charge-coupled device camera (Roper Scientific, Inc., Trenton, NJ, USA) mounted to the bottom port; a Xenon 150 W light source (OPTI QUIP, NY, USA) with a Hamamatsu C6979 power supply (Hamamatsu Photonics UK Ltd, Hertfordshire, UK) and; a Prior ProScan™II Controller (Prior Scientific, Inc., Cambridge, UK) for automated control of the microscope stage, shutters and filter wheels were driven by MetaMorph image processing software (Universal Imaging Corp., Donnington, PA, USA).

Time-lapse imaging of oocytes expressing GFP or hMad2-GFP was performed in stage-fitted dishes containing pre-warmed microdrops of M16 medium under mineral oil maintained at ambient conditions of 5% CO_2 and 37°C by means of a modified stage-mounted incubator (Solent, Plymouth, UK) as described previously (Herbert *et al.*, 2003; Homer *et al.*, 2005). Two 12-bit images (one brightfield image and one fluorescence image) were collected every 20 min for up to 22 h using the 20×objective lens at fixed settings of 1×1 binning and 100 ms exposure times.

For fluorescence imaging of DNA in live oocytes, oocytes were bathed in Hoechst 33342 (10 μg/ml; Sigma, Poole, UK) for 15 min and imaged using the 20×objective lens. Images were processed using MetaMorph software and assembled into panels using Adobe Photoshop software (Adobe Systems, Inc., San Jose, CA, USA).

GFP calibration and estimation of GFP protein concentration

A calibration curve of green fluorescence against known concentrations of purified recombinant enhanced GFP (EGFP; Clontech, BD Biosciences, CA, USA) was generated as described previously (Levasseur and McDougall, 2000; Homer *et al.*, 2005). In brief, oocytes were microinjected with known concentrations of EGFP. The resulting average total oocyte fluorescence intensity was estimated using MetaMorph software by drawing a region of interest over the entire oocyte which was then background-corrected by subtracting the mean fluorescence value of a cell-free region. From these data, a calibration curve of EGFP concentration versus oocyte fluorescence was generated. Since MmGFP is known to have the same spectral properties as EGFP, the intracellular concentration of translated MmGFP or MmGFP-tagged proteins such as hMad2-GFP could be easily estimated from the calibration curve based on oocyte fluorescence. Fluorescence images of oocytes microinjected with EGFP, GFP mRNA or hMad2-GFP mRNA were captured at 20× magnification on the fluorescence work station described above at the same settings used for time-lapse imaging.

mMad2: 539 5′— AAGTCCGTCTACGCTCATTTA — 3′ 559
hMad2: 539 5′— AAGTCCGCCTTCGTTCATTTA — 3′ 559

Figure 1. Nucleotide (nt) composition of the human *hMad2* coding sequence targeted by si539 (*hMad2*; nts 539–559). The aligned nt sequence of mouse *mMad2* (*mMad2*; nts 539–559) is also shown. The 3-nt differences between the two sequences are highlighted by boxes.

siRNA design, synthesis and analysis

ds siRNAs were designed and synthesized by *in vitro* transcription using the *Silencer*™ siRNA Construction Kit (Ambion, Inc., Austin, TX, USA) according to the manufacturer's guidelines as summarized in the following steps: (1) Sequence design. The targeting sequence for *hMad2* (GenBank accession no. AJ000186; Li and Benezra, 1996) corresponded to nts 539–559 of the coding region relative to the first nt of the ATG start codon (Figure 1). This sequence was selected by first scanning the length of the *hMad2* gene for AA sequences and then choosing a 21-nt sequence comprising the AA and downstream 19-nts which lacked significant homology to any human gene and which also possessed a GC content below 50% as this increases susceptibility to siRNA-induced degradation (Elbashir *et al.*, 2001). (2) siRNA oligonucleotide template synthesis. Manufacture of the ds siRNA required that two DNA templates be synthesized and desalted (Invitrogen Ltd, Paisley, Scotland). The two 29-nt DNA templates were comprised of 21-nts encoding the hMad2-targeting siRNA and an 8-nt sequence complementary to a T7 promoter primer (5′-CCTGTCTC-3′). The latter was important to overcome the sequence restrictions required for efficient T7 polymerase-mediated *in vitro* transcription which would otherwise severely limit the number of potential target mRNA sequences. DNA templates were hybridized for 5 min at 70°C to a T7 Promoter Primer supplied with the kit consisting of a T7 promoter sequence and an 8-nt sequence complimentary to the 8-nts within the siRNA transcription templates. The 3′ ends of the hybridized oligonucleotides were then extended using the Klenow fragment of DNA polymerase for 30 min at 37°C to create ds templates for siRNA transcription. (3) Manufacture of siRNAs by *in vitro* transcription. Following T7 promoter-driven *in vitro* transcription for 2 h at 37°C, the resulting RNA transcripts were hybridized overnight at 37°C to produce dsRNA now consisting of 5′ terminal leader sequences, a 19-nt target-specific dsRNA, and 3′ terminal UUs. The DNA templates and the 5′ leader sequences were removed by incubation at 37°C for 2 h with a DNase and a single-strand specific RNase which does not cleave UU residues thereby producing an siRNA with UU dinucleotide overhangs. (4) siRNA purification and analysis. Glass fibre filter binding was used for purification following which siRNAs were eluted into nuclease-free water to produce stock concentrations of 350 μg/ml as quantified by absorbance at 260 nm. Five microlitres of siRNA products were analysed by electrophoresis at 200 V in TBE (0.09 M Tris base, 0.09 M Boric acid, 2 mM of 0.5 M EDTA) using a non-denaturing 12% polyacrylamide gel.

In addition to si539, we synthesized a control siRNA designated GAPDHsi which was designed to target GAPDH, the DNA templates for which were supplied with the kit.

For microinjection, stock solutions were diluted 10-fold in nuclease-free water. The concentration of siRNAs used in this study was no higher than those reported for dsRNA in other studies. In our experiments, the final molar oocyte concentration of si539 was six times less than that of the siRNAs utilized to knockdown *Oct-3/4* and c-*mos* (Kim *et al.*, 2002) and two-thirds the concentration of the much longer dsRNAs utilized to suppress *MmGFP*, *E-cadherin* and c-*mos* in mouse oocytes and embryos (Wianny and Zernicka-Goetz, 2000). We are confident of efficient delivery of siRNAs as oocytes were individually microinjected to ~5% total oocyte volume determinable by the dispersal of ooplasm. We have previously demonstrated in mouse oocytes that microinjection is an effective means of achieving uniform gene silencing (Homer *et al.*, 2005).

Immufluorescence

Oocytes were fixed and permeabilized for 1 h in 4% paraformaldehyde and 0.3% Triton X-100 in phosphate-buffered saline (PBS). After three 15 min washes in PBS containing 4% bovine serum albumin (PBA), oocytes were blocked for 45 min in 10% goat serum in PBS. Following an overnight incubation with the mouse monoclonal antibody against β-tubulin (T-4026; Sigma, Poole, UK) in microdrops under oil at 4°C, oocytes were given three 15 min washes in PBA followed by a 45 min incubation in fluorescein isothiocyanate (FITC)-conjugated rabbit anti-mouse immunoglobulin G

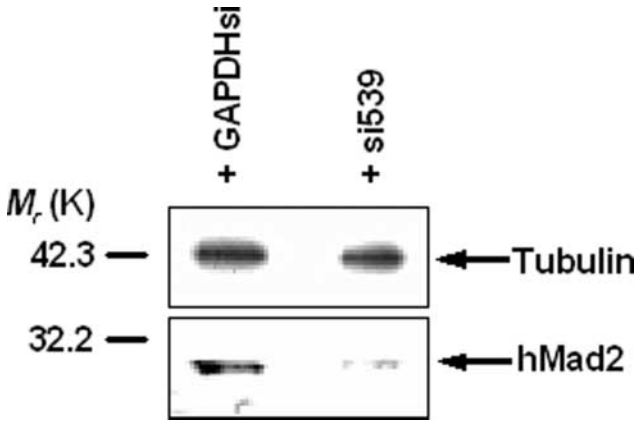

Figure 2. Evaluating si539 by Western blot analysis of human oocytes. GV-stage human oocytes were microinjected with either 35 μg/ml si539 ($n = 5$) or 35 μg/ml GAPDHsi ($n = 5$) and immunoblotted for hMad2 after 48 h of *in vitro* culture. Membranes were directly re-probed for α-tubulin as described previously (Liao *et al.*, 2000; Homer *et al.*, 2005) to check for equal loading of protein.

(F-5262; Sigma, Poole, UK) in microdrops under oil at room temperature. After a further three 15 min washes in PBA, DNA was stained with propidium iodide (200 μg/ml) in PBS for 20 min. Following another three 15 min washes in PBA, oocytes were transferred in volumes of approximately 10–20 μl to poly-L-lysine-coated glass slides scored beforehand with a diamond scriber to aid in locating fixed oocytes and mounted in 90% glycerol in PBS under a coverslip. Images were captured on the fluorescence workstation described above using the 40 × objective lens. Images were processed using MetaMorph software and assembled into panels using Adobe Photoshop.

Results

The function of a given gene is ultimately determined by the activity of its cognate protein. It follows that for very stable proteins, depletion of their corresponding mRNAs is not guaranteed to silence gene function due to persistence of pre-formed protein (Medema, 2004). Thus, in order to reliably evaluate the gene-silencing capability of a given RNAi tool, it is important to measure

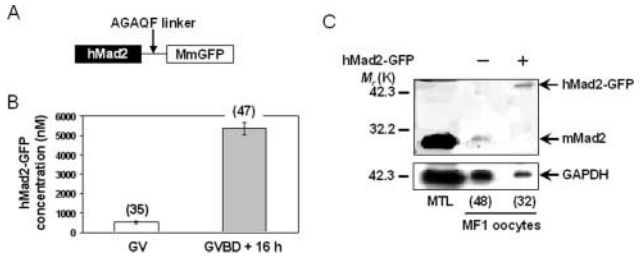

Figure 3. Expression of hMad2-GFP and mMad2 in MF1 mouse oocytes. (**A**) Schematic map of the hMad2 coupled C-terminally to MmGFP. (**B**) GV-stage mouse oocytes were microinjected with hMad2-GFP mRNA (1 μg/μl) and either maintained in dbcAMP-supplemented medium to prevent GVBD or cultured in standard medium until 16 h post-GVBD. GFP fluorescence was then assessed for each group from which the concentration of hMad2-GFP was estimated using a calibration curve described previously (Levasseur and McDougall, 2000; Homer *et al.*, 2005). The data shown represents the Mean ± SEM from four separate experiments. Statistical analysis was by Student's two-tailed *t*-test. Total oocyte numbers are shown in parentheses. (**C**) Western blot analysis of hMad2-GFP and mMad2. GV-stage oocytes were injected with hMad2-GFP mRNA (1 μg/μl), matured *in vitro* until 16 h post-GVBD and immunoblotted for Mad2 along with uninjected oocytes matured for an equivalent period. The anti-Mad2 antibody used recognized hMad2 and mMad2 with equal affinity. Membranes were directly re-probed for GAPDH as described above to check for equal loading of protein. Five microlitres of mouse testes lysate (MTL) served as a positive control. Total oocyte numbers per lane are shown in parentheses.

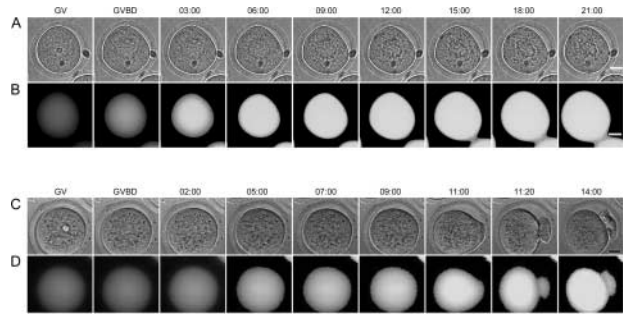

Figure 4. Effect of hMad2-GFP and GFP overexpression on progression through meiosis I. GV-stage mouse oocytes were microinjected with either hMad2-GFP mRNA (1 μg/μl; $n = 7$; **A** and **B**) or GFP mRNA (1 μg/μl; $n = 10$; **C** and **D**) and examined by time-lapse fluorescence microscopy. Brightfield (**A** and **C**) and fluorescence (**B** and **D**) images were captured at 20 min intervals for up to 21 h during which time oocytes were maintained at 37°C in 5% CO_2 by means of a stage-mounted Perspex incubator. Shown is one representative time-lapse series for each experimental group. Times post-GVBD above panels are depicted in h:min. Scale bars = 20 μM.

target protein levels. Therefore, we assessed si539 for its gene-silencing efficiency by measuring hMad2 protein levels in human oocytes using Western blotting. Previous work demonstrated that human oocytes expressed hMad2 and that this was readily detectable by immunoblotting (Homer *et al.*, 2005). Oocytes at the GV-stage were microinjected with either si539 ($n = 5$) or a non-silencing control siRNA (GAPDHsi; $n = 5$), matured *in vitro* for 48 h and then immunoblotted for Mad2 in two separate experiments (Figure 2). We found that the hMad2 signal from oocytes injected with si539 was 85–92% less intense that the signal from oocytes injected with GAPDHsi indicating that si539 efficiently reduced expression of hMad2 in human oocytes.

We sought further confirmation of silencing efficiency by utilizing a hMad2-GFP mRNA construct (Figure 3A) in mouse oocytes. We were able to estimate intracellular hMad2-GFP levels by relating oocyte fluorescence to a calibration curve derived using recombinant GFP protein as described previously (Levasseur and McDougall, 2000; Homer *et al.*, 2005). Mouse oocytes readily translated hMad2-GFP as mean levels increased roughly 10-fold by 16 h post-GVBD compared with levels at the GV-stage (Figure 3B) and Western blotting indicated that hMad2-GFP was expressed to levels above those of endogenous mMad2 (Figure 3C).

We and others have previously demonstrated that hMad2-GFP overexpression induces a meiosis I arrest in mouse oocytes (Wassmann *et al.*, 2003; Homer *et al.*, 2005) due to the inhibitory properties of Mad2. A previous dose–response analysis showed that ~1 μg/μl of hMad2-GFP mRNA consistently induced a meiosis I arrest; ~0.25 μg/μl did not alter the kinetics of meiosis I progression; and intermediate concentrations produced varying degrees of arrest (Homer *et al.*, 2005). Using our calibration curve, we examined the levels of hMad2-GFP that induced a complete meiosis I arrest more closely. We found that microinjecting ~1 μg/μl of hMad2-GFP mRNA resulted in an intra-oocyte concentration of hMad2-GFP above 5 μM and that this induced complete meiosis I arrest as indicated by the failure of first polar body extrusion (PBE) to occur, even beyond 20 h post-GVBD ($n = 7$; Figure 4A and B). In contrast, 8 of 10 (80%) oocytes expressing >5 μM GFP alone underwent PBE by about 11–12 h post-GVBD (Figure 4C and D) similar to the rate of PBE in wild-type oocytes (Figure 6B). DNA staining of live oocytes arrested by >5 μM hMad2-GFP revealed a single group of chromatin in a metaphase I-like configuration indicating that anaphase I was inhibited (Figure 5C and D). This

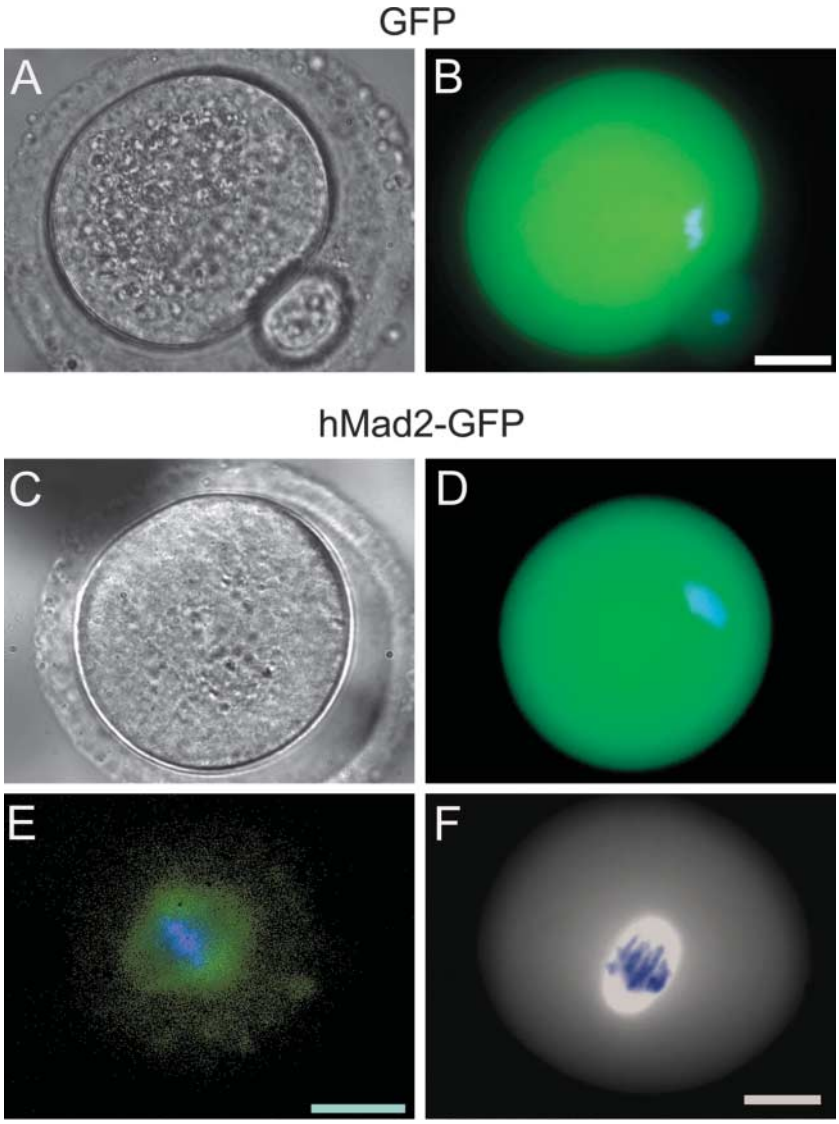

Figure 5. Overexpression of hMad2-GFP induces a metaphase I arrest. GV-stage mouse oocytes were microinjected with either GFP mRNA (1 μg/μl) or hMad2-GFP mRNA (1 μg/μl) to produce an intracellular concentration of GFP and hMad2-GFP >5 μM and cultured *in vitro* until 16 h post-GVBD. (**A**–**D**) Live oocytes expressing >5 μM of either GFP ($n = 10$; **A** and **B**) or hMad2-GFP ($n = 7$; **C** and **D**) were stained with Hoechst to highlight DNA (blue). Shown are brightfield (**A** and **C**) and fluorescence (**B** and **D**) images. (**E** and **F**) Spindle morphology in hMad2-GFP-arrested oocytes. Oocytes arrested by >5 μM hMad2-GFP were fixed using one of two techniques. In (**E**), oocytes were fixed following Triton-X extraction, stained with Hoechst and examined for fluorescence ($n = 7$). Shown is a merge of the GFP fluorescence and Hoechst (DNA) images. The spindle is outlined due to hMad2-GFP localization to microtubules (Howell *et al.*, 2000). In (**F**), following fixation/extraction, oocytes were double-stained using mouse anti-β-tubulin followed by FITC-labelled anti-mouse as the second layer to highlight the spindle (white) and propidium iodide (blue) to outline DNA. Shown is a merge of the FITC and propidium iodide images. Note that hMad2-GFP overexpression does not impair the assembly of bipolar spindles or chromosome congression to the equatorial region. Scale bars = 20 μm.

inhibitory effect of hMad2-GFP was due to hMad2 and not GFP as live oocytes expressing >5 μM GFP displayed two groups of DNA, one group in the oocyte and the other in the polar body, confirming that anaphase I had occurred (Figure 5A and B). The arrest induced by hMad2-GFP was not due to aberrant spindle assembly or impaired chromosome congression as oocytes arrested by >5 μM hMad2-GFP assembled a barrel-shaped spindle with chromosomes located at the equatorial region (Figure 5E and F). Therefore, >5 μM hMad2-GFP completely inhibited the metaphase I-to-anaphase I transition in mouse oocytes.

Next, we examined the effect of si539 on hMad2-GFP expression in mouse oocytes. Following microinjection with ~1 μg/μl of hMad2-GFP mRNA alone, oocytes translated a mean of 8.7 ± 2 μM hMad2-GFP by 16 h post-GVBD and consequently arrested in meiosis I ($n = 14$; Figure 6A and B). However, in the presence of si539, hMad2-GFP expression was reduced by ~94% to 0.5 ± 0.04 μM ($P = 0.003$; Figure 6A and C) with PBE occurring in ~70% of these oocytes similar to the rate in wild-type oocytes ($n = 9$; Figure 6B and C). This effect of si539 on hMad2-GFP was not a non-specific effect of *in vitro* transcribed siRNAs as oocytes co-injected with GAPDHsi and hMad2-GFP mRNA expressed similar levels of hMad2-GFP (7 ± 2.2 μM) to oocytes injected with hMad2-GFP mRNA alone (8.7 ± 2 μM; $P = 0.6$) and produced complete inhibition of PBE ($n = 7$; Figure 6A, B and E). si539 did not reduce expression from hMad2-GFP mRNA by targeting GFP as oocytes co-injected with si539 and GFP mRNA translated GFP (9 ± 1.8 μM) to levels that were similar to those of hMad2-GFP in oocytes injected with hMad2-GFP mRNA alone (8.7 ± 2 μM; $P = 0.89$) and, due to

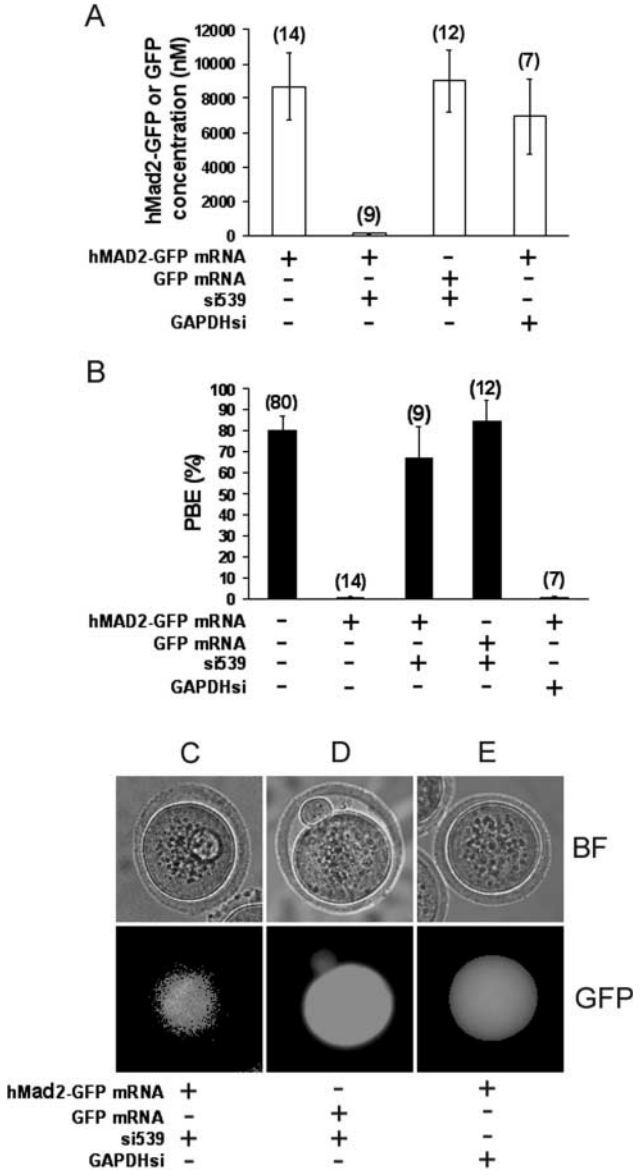

Figure 6. Evaluating the targeting efficiency of siRNAs based on fluorescence and PBE rates. GV-stage mouse oocytes were microinjected with the combinations of mRNAs and/or siRNAs as indicated in the figure and matured *in vitro* until 16 h post-GVBD. They were then assessed for green fluorescence intensity and for PBE. (**A**) hMad2-GFP or GFP protein concentrations were derived from oocyte fluorescence using a calibration curve as described previously and plotted graphically. hMad2-GFP and GFP concentrations are shown as the Mean ± SEM and were analysed statistically using the Student's two-tailed *t*-test. Total oocyte numbers are shown in parentheses. (**B**) PBE rates of oocytes represented in (**A**). The PBE rate for wild-type oocytes is shown for comparison. Total oocyte numbers are shown in parentheses. (**C**–**E**) Brightfield (BF) and fluorescence (GFP) images of representative oocytes from the three experimental groups indicated below panels.

the absence of linked hMad2, did not produce a meiosis I arrest ($n = 12$; Figure 6A, B and D). The silencing of si539 was highly specific as, in spite of only a 3-nt difference between hMad2 and mMad2 in the target sequence (Figure 1), si539 did not target endogenous mMad2 in mouse oocytes (Figure 7).

Therefore, overall si539 reduced expression from exogenous hMad2-GFP mRNA in mouse oocytes by targeting hMad2 resulting in reduced oocyte fluorescence and failure of meiosis I arrest. Importantly, the degree of knockdown of exogenous hMad2 mRNA estimated in mouse oocytes was very similar to the degree of

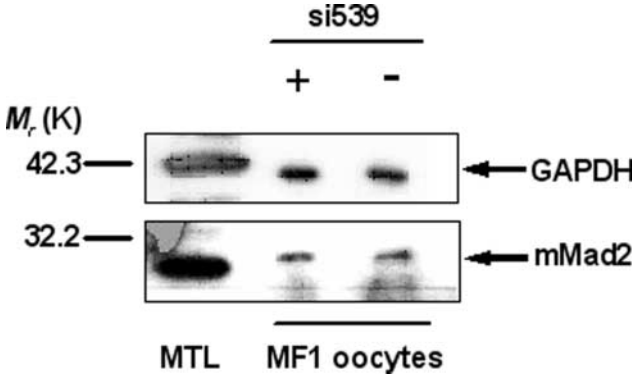

Figure 7. si539 does not target mMad2 in mouse oocytes. Ninety-one GV-stage mouse oocytes were microinjected with 35 μg/ml si539 and cultured *in vitro* until 16 h post-GVBD. si539-injected oocytes along with 91 uninjected control oocytes matured for an equivalent period were then immunoblotted for mMad2. Membranes were directly re-probed for GAPDH as described above to check for equal loading of protein while 5 μl of mouse testes lysate (MTL) served as a positive control.

knockdown of endogenous hMad2 in human oocytes. From this it can be inferred that the targeting efficiency of a given silencing tool intended for use in human oocytes can potentially be assayed using mouse oocytes.

Discussion

In the current study, we showed that human oocytes are amenable to RNAi-mediated gene knockdown. To our knowledge, this is the first such report and indicates that human oocytes possess the necessary cellular machinery for RNAi. Based on immunoblotting, we showed that si539 knocked down ~90% of hMad2 in human oocytes. This effect of si539 represented specific silencing of hMad2 for a number of reasons. Firstly, a control siRNA (GAPDHsi) did not affect hMad2 levels (Figure 2) indicating that the reduction of hMad2 by si539 was not a non-specific effect of *in vitro* transcribed siRNAs. Secondly, neither si539 nor GAPDHsi affected tubulin levels (Figure 2) implying that the reduction in hMad2 was not the consequence of global reduction in protein synthesis. Thirdly, si539 knocked down hMad2 (Figure 2) but not mMad2 (Figure 7). Given that there is only a 3-nt difference in the target sequence between the two genes (Figure 1), this reflects a highly specific effect of si539. Finally, using an exogenous GFP-tagged hMad2 mRNA in mouse oocytes, we conclusively showed that si539 specifically targeted hMad2 as discussed later in greater detail (Figure 6).

The reduced levels of hMad2 in the si539-injected group of human oocytes was not due to differences in oocyte populations between this group and the control group as we controlled for variables that might otherwise affect hMad2 protein levels. Firstly, previous data indicated that Mad2 levels increase as mouse oocytes undergo maturation *in vitro* (Homer *et al.*, 2005). Due to potential variation in hMad2 levels with duration in culture, therefore, we utilized only human oocytes which had undergone GVBD and which had been cultured *in vitro* for equivalent periods of time for immunoblot analysis. Secondly, lower levels of hMad2 mRNA transcripts in oocytes from older women compared with those from younger women (Steuerwald *et al.*, 2001) suggest that female age is another factor that could affect oocyte hMad2 protein levels. The lower hMad2 signal in oocytes treated with si539 compared with control oocytes was not related to female age, however, as mean age was similar for both groups of women (32 ± 5.2 versus 33 ± 4.8; $P = 0.8$).

A major obstacle to studying gene function during human female meiosis I remains the extreme paucity of immature human oocytes. Therefore, we sought to validate si539's targeting capability further using a GFP-based approach which would not necessitate the use of human oocytes. Mouse oocytes were shown to readily express an exogenous hMad2-GFP mRNA construct to levels in excess of endogenous mMad2 (Figure 3). Based on oocyte fluorescence levels, si539 was shown to effectively target hMad2-GFP mRNA in mouse oocytes as oocytes co-injected with si539 and hMad2-GFP mRNA exhibited minimal fluorescence (Figure 6). Based on the ability to relate GFP fluorescence to intracellular protein levels by means of a calibration curve (Levasseur and McDougall, 2000; Homer *et al.*, 2005), it was estimated that si539 reduced expression from exogenous hMad2-GFP mRNA by ~94% (Figure 6). This effect of si539 was specifically due to hMad2-targeting as neither GFP mRNA nor mMad2 was affected by si539 and a control siRNA did not target hMad2-GFP mRNA (Figures 6 and 7). Consistent with efficient knockdown, we showed that not only did si539 reduce oocyte fluorescence, it also rescued the meiosis I arrest otherwise induced by hMad2-GFP mRNA (Figure 6). We acknowledge that an easily reproducible phenotype is unlikely to be available for many of the genes for which function is being sought. However, this does not detract from the wider applicability of this approach as our use of the meiosis I arrest-phenotype served merely to confirm what had been deduced from other controlled experiments.

Accurate assignment of gene function based on RNAi is predicated on the assurance that silencing is exclusively restricted to the gene of interest thus making rigorous evaluation of potential sequences an essential prerequisite. As a given siRNA is not guaranteed to produce efficient knockdown, a large investment in research material may be required before one or more reliable sequences can be isolated from among a battery of potential candidates (Dykxhoorn *et al.*, 2003; Medema, 2004). Such an investment can cripple research efforts when the research material involved is in extremely limited supply as it is with human oocytes. In addition to utilizing mouse oocytes as described in this report, another option for reducing the drain on research material would be to employ other reverse-genetic approaches which are more likely to produce first-time silencing such as long dsRNAs or morpholinos. Long dsRNAs are complimentary to extensive stretches of target mRNA (Svoboda *et al.*, 2000; Wianny and Zernicka-Goetz, 2000; Lefebvre *et al.*, 2002) and, following intracellular cleavage by the Dicer endoribonuclease, generate a plethora of siRNAs (Dykxhoorn *et al.*, 2003) with a proportionately greater chance of producing silencing than a single siRNA duplex. One important caveat is that it is unknown whether or not dsRNAs longer than 30-nts will elicit in human oocytes an interferon response resulting in global down-regulation of protein translation as occurs in mammalian somatic cells (Dykxhoorn *et al.*, 2003; Medema, 2004). The lack of an interferon response to long dsRNA in mouse oocytes (Svoboda *et al.*, 2000) holds promise that this technique would prove to be applicable to human oocytes. An alternative to long dsRNAs are morpholinos that sterically block translation initiation by complimentary binding in the region of the AUG translation start site (Heasman, 2002). Morpholinos yield a high likelihood of silencing due to the restricted region of mRNA that is targeted and their high affinity for mRNA. Regardless of the reverse-genetic approach employed, systematic validation of targeting efficiency and selectivity is imperative.

It is envisioned that the experimental paradigm presented here can be incorporated into gene knockdown studies involving human oocytes in two scenarios. One possibility is to conduct the entire evaluation phase of a given gene-targeting tool using mouse oocytes. A significant drawback of such an approach is that efficient knockdown of an exogenous mRNA in mouse oocytes may not necessarily equate to a similar degree of silencing of endogenous mRNA in human oocytes. In spite of this, our data indicate that, in some cases at least, the mouse model can provide a reliable measure of the degree of endogenous gene silencing as immunoblotting demonstrated that si539 knocked down 85–92% of hMad2 in human oocytes (Figure 2) similar to the degree of knockdown (~94%) for exogenous hMad2 in mouse oocytes (Figure 6). Alternatively, both human and mouse oocytes might be used in tandem. For instance, RT–PCR-based techniques that can quantify mRNA in a single human oocyte (Steuerwald *et al.*, 2000) might allow preliminary evaluation of a given tool to be performed on human material. If this indicates that the mRNA of interest is reduced, more extensive control experiments aimed at assessing effects on protein expression can be performed using mouse oocytes. It is important to note that validating gene silencing based on RT–PCR alone can be misleading due to the imperfect correlation between mRNA and protein levels. This is particularly relevant to proteins with a very long half-life which may remain stable within the timeframe of an experiment in spite of a reduction in the levels of their cognate mRNA and also to those siRNAs which silence expression by repressing translation without producing significant mRNA degradation (Medema, 2004). Overall, regardless of the reverse-genetic approach that is favoured, we anticipate that a combined scheme for evaluating gene-targeting tools as suggested above will greatly facilitate human oocyte research.

Although comprehensive evaluation should ideally be conducted exclusively within the endogenous system, the extreme paucity of immature human oocytes dictates that novel and unconventional approaches need to be considered if progress is to be made in unravelling gene function during human female meiosis I. By facilitating the knockdown of genes in human oocytes, a modified approach to RNAi as suggested here can bring us closer to understanding the origins of disorders such as Down's syndrome and the molecular reasons for their age-related increase in incidence. Furthermore, expanding our understanding of the genetic regulation of oocyte maturation will doubtless assist in the advancement of burgeoning therapeutic options in reproductive medicine such as *in vitro* maturation of oocytes.

Acknowledgements

We thank J. Gurdon and R. Benezra for the generous gifts of pRN3 and plasmids. We acknowledge all members of the laboratory for technical assistance and advice. This work was supported by a WellBeing Research Training Fellowship to H.A.H. (RTF/387) and Project Grants from Newcastle University Hospitals Special Trustees to M.H. and the Wellcome Trust to A.M.D.

References

Bernard P, Maure JF and Javerzat JP (2001) Fission yeast Bub1 is essential in setting up the meiotic pattern of chromosome segregation. Nat Cell Biol 3,522–526.

Dykxhoorn DM, Novina CD and Sharp PA (2003) Killing the messenger: short RNAs that silence gene expression. Nat Rev Mol Cell Biol 4, 457–467.

Elbashir SM, Harboth J, Lendeckel W, Yalcin A, Weber K and Tuschl T (2001) Duplexes of 21-nucleotide RNAs mediate RNA interference in cultured mammalian cells. Nature 411,494–498.

Fedoriw AM, Stein P, Svoboda P, Schultz RM and Bartolomei MS (2004) Transgenic RNAi reveals essential function for CTCF in H19 gene imprinting. Science 303,238–240.

Fenwick J, Platteau P, Murdoch AP and Herbert M (2002) Time from insemination to first cleavage predicts developmental competence of human preimplantation embryos *in vitro*. Hum Reprod 17,407–412.

Hassold T and Hunt P (2001) To err (meiotically) is human: the genesis of human aneuploidy. Nat Rev Genet 2,280–291.

Heasman J (2002) Morpholino oligos: making sense of antisense? Dev Biol 243,209–214.

Herbert M, Levasseur M, Homer H, Yallop K, Murdoch A and McDougall A (2003) Homologue disjunction in mouse oocytes requires proteolysis of securin and cyclin B1. Nat Cell Biol 5,1023–1025.

Homer HA, McDougall A, Levasseur M, Yallop K, Murdoch AP and Herbert M (2005) Mad2 prevents aneuploidy and premature proteolysis of cyclin B and securin during meiosis I in mouse oocytes. Genes Dev 19,202–207.

Howell BJ, Hoffman DB, Fang G, Murray AW and Salmon ED (2000) Visualization of Mad2 dynamics at kinetochores, along spindle fibers, and at spindle poles in living cells. J Cell Biol 150,1233–1249.

Kim MH, Yuan X, Okumura S and Ishikawa F (2002) Successful inactivation of endogenous *Oct-3/4* and c-*mos* genes in mouse preimplantation embryos and oocytes using short interfering RNAs. Biochem Biophys Res Comm 296,1372–1377.

Ledan E, Polanski Z, Terret ME and Maro B (2001) Meiotic maturation of the mouse oocyte requires an equilibrium between cyclin B synthesis and degradation. Dev Biol 232,400–413.

Lefebvre C, Terret ME, Djiane A, Rassinier P, Maro B and Verlhac MH (2002) Meiotic spindle stability depends on MAPK-interacting and spindle-stabilizing protein (MISS), a new MAPK substrate. J Cell Biol 157, 603–613.

Lemaire P, Garrett N and Gurdon JB (1995) Expression cloning of Siamois, a new Xenopus homeobox gene expressed in dorsal vegetal cells of blastulae and capable of inducing a complete secondary axis. Cell 81,85–94.

Levasseur M and McDougall A (2000) Sperm-induced calcium oscillations at fertilisation in ascidians are controlled by cyclin B1-dependent kinase activity. Development 127,631–641.

Li Y and Benezra R (1996) Identification of a human mitotic checkpoint gene: hsMAD2. Science 274,246–248.

Liao J, Xu X and Wargovich M (2000) Direct reprobing with anti-beta-actin antibody as an internal control for western blot analysis. Biotechniques 28,216–218.

Medema RH (2004) Optimizing RNA interference for application in mammalian cells. Biochem J 380,593–603.

Mussachio A and Hardwick K (2002) The spindle checkpoint: structural insights into dynamic signalling. Nat Rev Mol Cell Biol 3,731–741.

Peters JM (2002) The anaphase-promoting complex: proteolysis in mitosis and beyond. Mol Cell 9,931–943.

Poss KD, Nechiporuk A, Stringer KF, Lee C and Keating MT (2004) Germ cell aneuploidy in zebrafish with mutations in the mitotic checkpoint gene *mps1*. Genes Dev 18,1527–1532.

Shonn MA, McCarroll R and Murray AW (2000) Requirement of the spindle checkpoint for proper chromosome segregation in budding yeast meiosis. Science 289,300–303.

Stein P, Svoboda P, Anger M and Schultz RM (2003a) RNAi: mammalian oocytes do it without RNA-dependent RNA polymerase. RNA 9,187–192.

Stein P, Svoboda P and Schultz RM (2003b) Transgenic RNAi in mouse oocytes: a simple and fast approach to study gene function. Dev Biol 256, 187–193.

Steuerwald N, Cohen J, Herrera RJ and Brenner C (2000) Quantification of mRNA in single oocytes and embryos by real-time rapid cycle fluorescence monitored RT–PCR. Mol Hum Reprod 6,448–453.

Steuerwald N, Cohen J, Herera RJ, Sandalinas M and Brenner CA (2001) Association between spindle assembly checkpoint expression and maternal age in human oocytes. Mol Hum Reprod 7,49–55.

Svoboda P, Stein P, Hayashi H and Schultz RM (2000) Selective reduction of dormant maternal mRNAs in mouse oocytes by RNA interference. Development 127,4147–4156.

Tulac S, Dosiou C, Suchanek E and Giudice LC (2004) Silencing lamin A/C in human endometrial stromal cells: a model to investigate endometral gene function and regulation. Mol Hum Reprod 10,705–711.

Wassmann K, Niault T and Maro B (2003) Metaphase I arrest upon activation of the MAD2-dependent spindle checkpoint in mouse oocytes. Curr Biol 13,1596–1608.

Wianny F and Zernicka-Goetz M (2000) Specific interference with gene function by double-stranded RNA in early mouse development. Nat Cell Biol 2,70–75.

Yu J, Deng M, Medvedev S, Yang J, Hecht NB and Schultz RM (2004) Transgenic RNAi-mediated reduction of MSY2 in mouse oocytes results in reduced fertility. Dev Biol 268,195–206.

Zernicka-Goetz M, Pines J, McLean Hunter S, Dixon JP, Siemering KR, Haseloff J and Evans MJ (1997) Following cell fate in the living mouse embryo. Development 124,1133–1137.

Submitted on February 26, 2005; accepted on April 26, 2005